J|A|C|S COMMUNICATIONS

Published on Web 01/06/2010

The Structural Basis of *Cryptosporidium*-Specific IMP Dehydrogenase Inhibitor Selectivity

Iain S. MacPherson,[†] Sivapriya Kirubakaran,[†] Suresh Kumar Gorla,[†] Thomas V. Riera,[‡] J. Alejandro D'Aquino,[‡] Minjia Zhang,[†] Gregory D. Cuny,[⊥] and Lizbeth Hedstrom*[,†,§]

Departments of Biology, Biochemistry, and Chemistry, Brandeis University, MS009, 415 South Street, Waltham, Massachusetts 02454, and Laboratory for Drug Discovery in Neurodegeneration, Brigham & Women's Hospital, Harvard Medical School, 65 Landsdowne Street, Cambridge, Massachusetts 02139

Received November 24, 2009; E-mail: hedstrom@brandeis.edu

Cryptosporidium spp. are a major cause of the "vicious cycle" of diarrhea and malnutrition in the developing world and a potential bioterrorism agent.[1,2] This disease is prolonged and life-threatening in immuno-compromised patients. Currently, no effective therapy exists for *Cryptosporidium* infections. The parasite obtains guanine nucleotides via a streamlined pathway that requires inosine 5′-monophosphate dehydrogenase (IMPDH).[3−5] Curiously, the gene encoding *Cp*IMPDH appears to have been obtained from a bacteria via lateral gene transfer.[6,7] We have exploited this unexpected divergence of parasite and host enzymes to identify *Cp*IMPDH-specific inhibitors in a high-throughput screen.[8] Here we report X-ray crystal structures of *Cp*IMPDH that explain the selectivity of one inhibitor series and use this information to design more potent and selective analogues.

Recombinant *Cp*IMPDH was purified as described previously[9] and crystallized using the hanging drop vapor diffusion method. Protein solution (4 mg/mL IMPDH, 50 mM Tris-HCl, pH 7.5, 150 mM KCl, 5% glycerol, and 2 mM DTT) was mixed with well solution (34% PEG 4000, 25 mM sodium acetate, and 100 mM Tris-HCl, pH 8.5) in a 1:1 ratio. Data were collected from a single crystal at 100 K at beamline 8-BM at Advanced Photon Source (Argonne National Laboratory, Argonne, IL). The crystals had the symmetry of space group $P2_12_12$. The asymmetric unit contains one tetramer, which is the active form of IMPDH.[12] The structure was solved to 3.2 Å resolution ($R = 27\%$, $R_{free} = 33\%$) by molecular replacement using the structure of IMPDH from *Borrelia burgdorferi* (PDB accession 1EEP[10]) as a search model.[11] Only 301 of 400 residues are visible in the most structured monomer; the disordered regions include catalytically important segments 214−222, 299−333, and 380−400 as well as residues 92−122, which are not required for enzymatic activity.[12] Unfortunately, we were unable to improve this crystal form. This structure has been deposited in the PDB (3FFS).

To facilitate crystallization, residues 90−134 were replaced with SerGlyGly;[11] this modification has no effect on enzymatic activity (Figure S1, Supporting Information). A crystallization screen was performed in the presence of IMP and various inhibitors that emerged from initial evaluation of the SAR. Compound **C64** was a particularly attractive candidate for crystallization because of its improved potency relative to that of the parent compound **C** and the presence of a bromine atom which would allow the two aromatic groups to be easily distinguished (Table 1). Crystals were obtained in the presence of saturating concentrations of inhibitor **C64** (20 μM), IMP (1 mM), 100 mM sodium acetate, pH 4.6, 20 mM $CaCl_2$, and 30% MPD under oil. These crystals had the symmetry of space group $P2_1$ with two tetramers in the asymmetric unit. Data were collected at a wavelength of 0.9194 Å, enabling the simultaneous collection of bromine k-edge anomalous dispersion data. The structure was solved by molecular replacement to 2.8 Å resolution using the native *Cp*IMPDH structure as the starting model ($R =$ 22.4%, $R_{free} = 26.6\%$).

Table 1. Inhibition of *Cp*IMPDH and hIMPDH2

Cmpd	R_1	R_2	IC_{50} (nM)	
			*Cp*IMPDH	hIMPDH2
C	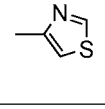	4-OMePh	1200 ± 200 [a]	≥200,000 [a,b]
C10		4-ClPh	120 ± 40	≥20,000 [c]
C14		4-BrPh	60 ± 30	≥20,000 [c]
C86		2,3-di-ClPh	30 ± 10	≥40,000 [d]
C90		2-Naph	7 ± 4	≥40,000 [d]
C61	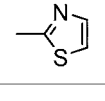	4-ClPh	30 ± 10	≥40,000 [d]
C64		4-BrPh	28 ± 9	≥40,000 [d]
C84		2,3-di-ClPh	18 ± 5	≥8,000 [c]
C97		2-Naph	8 ± 3	≥40,000 [d]

[a] Values from ref 8. [b] ≤20% inhibition at 50 μM. [c] ≤20% inhibition at 5 μM. [d] ≤10% inhibition at 5 μM. [e] ≤20% inhibition observed at 2 μM.

While the overall structure of the E·IMP·**C64** complex is similar to that of the unliganded enzyme, several additional residues are observed. Residues 214−226, which include the catalytic Cys219, are observed in most of the monomers, as are parts of the active-site flap (residues 302−330) containing the characteristic ArgTyr motif.[12] Lastly, the SerGlyGly linker is visible in all monomers. Electron density for IMP is observed in all eight monomers. Monomers B, D, and H contained extra electron density near IMP (Figure 1). Bromine k-edge anomalous dispersion maps allowed the unambiguous assignment of the bromine atom in **C64** in all three monomers. The rest of **C64** was modeled into the remaining electron density; similar conformations of **C64** are obtained in all three monomers. This structure has been deposited in the PDB (3KHJ).

Surprisingly, **C64** binds in an unprecedented fashion. Inhibitors of human IMPDH2 such as mycophenolic acid and merimepodib bind in the nicotinamide subsite, stacking against the purine ring of IMP in a parallel fashion, and extend either into the NAD site or into a pocket adjacent the active site but within the same monomer.[12−14] In contrast, the thiazole ring of **C64** stacks against the purine ring of IMP perpendicularly, and the remainder of **C64** extends across the subunit interface into a pocket in the adjacent monomer, where the bromoaniline moiety interacts with Tyr358′ (where ′ denotes a residue from the adjacent subunit; Figure 2). This residue forms a hydrogen-bonding network involving Glu329, Ser354, Thr221, and possibly the amide nitrogen of **C64** (Figure

[†] Department of Biology, Brandeis University.
[‡] Department of Biochemistry, Brandeis University.
[§] Department of Chemistry, Brandeis University.
[⊥] Brigham & Women's Hospital.

 10.1021/ja909947a

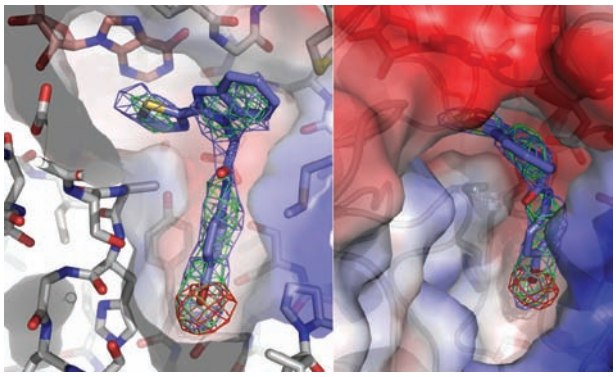

Figure 1. Co-crystallized structure of *Cp*IMPDH (light gray) with IMP (salmon) and **C64** (slate) shown from two different perspectives. The electron density map prior to **C64** modeling with coefficients $2F_o - F_c$ is contoured to 1σ and shown as a slate cage. The electron density map prior to **C64** modeling with coefficients $F_o - F_c$ is contoured to 3σ and shown as a green cage. Bromine k-edge peak anomalous dispersion map is contoured to 4σ and shown as a red cage. The red and blue surfaces denote regions of negative and positive electrostatic potential, respectively.

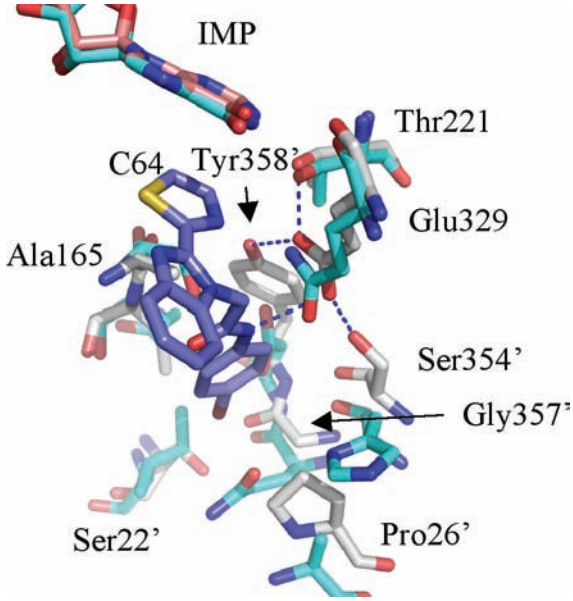

Figure 2. **C64** binding pocket of *Cp*IMPDH (light gray) superposed with human IMPDH2 (cyan). *Cp*IMPDH residues are labeled.

2). Ser22′, Pro26′, Ala165, Gly357′ form the remainder of the inhibitor binding pocket. With the exception of Thr221, all of these residues are different in human IMPDHs (Figure 2). Thus, these interactions account for the selectivity of **C64** for *Cp*IMPDH over human IMPDHs.

The structure also revealed the presence of a cavity adjacent to the bromoaniline moiety (Figure 1), which suggested that more potent inhibitors might be created by increasing the bulk of this substituent. Additional benzimidazole based inhibitors were prepared by condensing *o*-phenylenediamine **1** with thiazole carboxaldehydes **2** in the presence of the oxidizing reagent sodium metabisulfite **3** (Scheme 1).[15] The resulting 2-substituted benzimidazoles **4** were then coupled with different bromoacetylamides **5** under mild basic conditions to give the new analogues **6** (Table 1).

The *Cp*IMPDH inhibitory activity of the compounds was assessed by monitoring the production of NADH by fluorescence (Table 1).[16] Replacing the *p*-MeO of the parent compound **C** with

Scheme 1. Synthesis of inhibitors

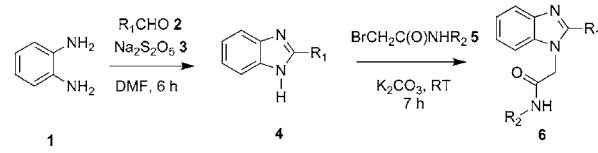

Cl or Br increased potency by 10-fold (**C10**) and 20-fold (**C14**), respectively, as has been similarly observed with another inhibitor series.[16] To fill the cavity observed in the crystal structure, the para-substituted aniline group was replaced with 3,4-dichloroaniline (**C86**) or 2-naphthylamine (**C90**); the addition of a second Cl improved potency by a factor of 2, whereas fusing an additional aromatic ring increased potency by a factor of 8. Similar trends were observed when the thiazole ring was attached at the 2-position (**C61**, **C64**, **C84**, and **C90**). None of the compounds displayed significant inhibitory activity against human IMPDH2. The best *Cp*IMPDH inhibitor, **C90**, has an $IC_{50} = 7.4$ nM with selectivity $>10^3$ for the parasite enzyme.

In conclusion, the crystal structure of *Cp*IMPDH reveals the structural basis of inhibitor selectivity and a strategy for further optimization. This information was used to design more potent and selective inhibitors of *Cp*IMPDH that are potential lead compounds for the treatment of cryptosporidiosis.

Acknowledgment. This work was supported by funding from NIH/NIAID (U01AI075466 to L.H. and RR15301 to APS). G.D.C. thanks NERCE/BEID, the Harvard NeuroDiscovery Center, and the Partners Center for Drug Discovery for financial support. Initial crystal screening was performed at the Hauptman Woodward Institute. We thank Jennifer Lu for assistance in crystallizing *Cp*IMPDH, Kene Piasta and the staff at APS for data collection, and our colleague Gregory Petsko for advice and comments on the manuscript.

Supporting Information Available: Methods, crystallographic data table, spectra, chromatograms and complete refs 4 and 5. This material is available free of charge via the Internet at http://pubs.acs.org.

References

(1) Fayer, R. *Vet. Parasitol.* **2004**, *126*, 37–56.
(2) Huang, D. B.; White, A. C. *Gastroenterol. Clin. North Am.* **2006**, *35*, 291–314, viii.
(3) Striepen, B.; Pruijssers, A. J.; Huang, J.; Li, C.; Gubbels, M. J.; Umejiego, N. N.; Hedstrom, L.; Kissinger, J. C. *Proc. Natl. Acad. Sci. U.S.A.* **2004**, *101*, 3154–9.
(4) Abrahamsen, M. S.; et al. *Science* **2004**, *304*, 441–445.
(5) Xu, P.; et al. *Nature* **2004**, *431*, 1107–1112.
(6) Striepen, B.; White, M. W.; Li, C.; Guerini, M. N.; Malik, S. B.; Logsdon, J. M., Jr.; Liu, C.; Abrahamsen, M. S. *Proc. Natl. Acad. Sci. U.S.A.* **2002**, *99*, 6304–6309.
(7) Umejiego, N. N.; Li, C.; Riera, T.; Hedstrom, L.; Striepen, B. *J. Biol. Chem.* **2004**, *279*, 40320–40327.
(8) Umejiego, N. N.; Gollapalli, D.; Sharling, L.; Volftsun, A.; Lu, J.; Benjamin, N. N.; Stroupe, A. H.; Riera, T. V.; Striepen, B.; Hedstrom, L. *Chem. Biol* **2008**, *15*, 70–77.
(9) Riera, T. V.; Wang, W.; Josephine, H. R.; Hedstrom, L. *Biochemistry* **2008**, *47*, 8689–96.
(10) McMillan, F. M.; Cahoon, M.; White, A.; Hedstrom, L.; Petsko, G. A.; Ringe, D. *Biochemistry* **2000**, *39*, 4533–4542.
(11) See Supporting Information for details.
(12) Hedstrom, L. *Chem. Rev.* **2009**, *109*, 2903–2928.
(13) Sintchak, M. D.; Fleming, M. A.; Futer, O.; Raybuck, S. A.; Chambers, S. P.; Caron, P. R.; Murcko, M.; Wilson, K. P. *Cell* **1996**, *85*, 921–930.
(14) Sintchak, M. D.; Nimmesgern, E. *Immunopharmacology* **2000**, *47*, 163–184.
(15) Yang, D.; Fokas, D.; Li, J.; Yu, L.; Baldino, C. M. *Synthesis* **2005**, 47–56.
(16) Maurya, S. K.; Gollapalli, D. R.; Kirubakaran, S.; Zhang, M.; Johnson, C. R.; Benjamin, N. N.; Hedstrom, L.; Cuny, G. D. *J. Med. Chem.* **2009**, *52*, 4623–30.

JA909947A